Estimation of the poroelastic parameters of cortical bone

Theo H. Smit[a,*], Jacques M. Huyghe[b], Stephen C. Cowin[c]

[a] *Department of Clinical Physics and Informatics, Medical Centre Vrije Universiteit, PO Box 7057, 1007 MB Amsterdam, Netherlands*
[b] *Department of Mechanical Engineering, Eindhoven University of Technology, Netherlands*
[c] *New York Centre for Biomedical Engineering and Department of Mechanical Engineering, City University of New York, USA*

Abstract

Cortical bone has two systems of interconnected channels. The largest of these is the vascular porosity consisting of Haversian and Volkmann's canals, with a diameter of about 50 μm, which contains a.o. blood vessels and nerves. The smaller is the system consisting of the canaliculi and lacunae: the canaliculi are at the submicron level and house the protrusions of the osteocytes. When bone is differentially loaded, fluids within the solid matrix sustain a pressure gradient that drives a flow. It is generally assumed that the flow of extracellular fluid around osteocytes plays an important role not only in the nutrition of these cells, but also in the bone's mechanosensory system.

The interaction between the deformation of the bone matrix and the flow of fluid can be modelled using Biot's theory of poroelasticity. However, due to the inhomogeneity of the bone matrix and the scale of the porosities, it is not possible to experimentally determine all the parameters that are needed for numerical implementation. The purpose of this paper is to derive these parameters using composite modelling and experimental data from literature. A full set of constants is estimated for a linear isotropic description of cortical bone as a two-level porous medium. Bone, however, has a wide variety of mechanical and structural properties; with the theoretical relationships described in this note, poroelastic parameters can be derived for other bone types using their specific experimental data sets. © 2002 Elsevier Science Ltd. All rights reserved.

Keywords: Poroelasticity; Cortical bone; Fluid flow; Biot's theory; Mechanosensitivity; Permeability

1. Introduction

Cortical bone contains a hierarchical structure of interconnected channels (Gray's Anatomy, 1996). At the highest level, Haversian and Volkmann's canals with a diameter of about 50 μm house (a.o.) blood vessels and nerves. Canaliculi are two orders of magnitude smaller and contain the osteocytic protrusions. Being open to the vascular canals, canaliculi form a passage for nutrients and other molecules travelling to and from the osteocytes. Mechanical loading enhances the exchange of molecules by driving the free fluid in and out (Piekarski and Munro, 1977; Wang et al., 2000). Fluid flow has also been suggested to play a role in the mechanosensory system of bone (Weinbaum et al, 1991; Cowin et al., 1995; Burger et al., 1998): osteocytes thereby would be stimulated by fluid shear stress and

subsequently produce signalling molecules directing the osteoclasts and osteoblasts at the bone surface. A better understanding of this mechanism is important for bone-related clinical problems such as osteoporosis and the fixation of implants.

The relation between matrix deformation and fluid flow can be described by Biot's theory of poroelasticity (Biot, 1941, 1955). The kinematic quantities in this approach are displacement vector u_i, tracking the movement of the porous solid, and vector q_i, describing the flux of fluid mass. The field variables are total stress σ_{ij}, strain in the solid phase ε_{ij}, fluid (pore) pressure p, and specific fluid volume ζ. Strain quantities ε_{ij} and ζ are related to the displacement quantities u_i and q_i according to

$$\varepsilon_{ij} = \tfrac{1}{2}(u_{i,j} + u_{j,i}) \tag{1}$$

and the fluid mass balance

$$\frac{\partial \zeta}{\partial t} = q_{k,k}, \tag{2}$$

*Corresponding author. Tel.: +31-20-4441245; fax: +31-20-4444147.

E-mail address: th.smit@vumc.nl (T.H. Smit).

Nomenclature

B	Skempton pore pressure coefficient
E	Young's modulus
G	shear modulus
K	bulk modulus
k	intrinsic (geometric) permeability
p	pore pressure
q	fluid flow
t	time
u	displacement of the solid
α	Biot effective stress coefficient
ε	strain
φ	pore volume fraction
κ	hydraulic permeability, equal to k/μ
μ	dynamic fluid viscosity

σ	stress
τ_{r}	relaxation time
v	Poisson's ratio
ζ	variation of unstrained fluid volume per unit volume of the porous material (fluid content)

Subscripts

i, j, k	components of the tensors in the field equations
d	drained situation
u	undrained situation
lc	lacuno-canalicular level
v	vascular level
f	fluid phase
s	solid phase

where t represents time. Darcy's law relates mass flux q_i to the gradient of pore pressure p:

$$q_i = -\kappa p \delta_{ij}, \tag{3}$$

where κ is the hydraulic permeability coefficient. κ is further defined by $\kappa = k/\mu$, with k being the intrinsic permeability and μ the fluid's dynamic viscosity. k is a function of the pore geometry, more particularly the connectedness of the porosity φ and the size and spatial arrangement of the pores.

Biot's theory further includes constitutive equations of the solid structure. Although bone is anisotropic with respect to its elastic moduli and permeability, both are considered isotropic here, because the anisotropic poroelastic bone constants have not yet been determined, and bones and osteons are almost isotropic in their transverse planes, which is where fluid flow mainly occurs. To describe the poroelastic problem, the stress–strain relations of the theory of elasticity are extended with the pressure component (Biot, 1941):

$$\sigma_{ij} + \alpha p \delta_{ij} = 2G_{\mathrm{d}}\varepsilon_{ij} + \left(\frac{2G_{\mathrm{d}}v_{\mathrm{d}}}{1 - 2v_{\mathrm{d}}}\right)\varepsilon_{kk}\delta_{ij}, \tag{4}$$

where G_{d} and v_{d} are the drained shear modulus and Poisson's ratio of the solid, and α the Biot effective stress coefficient. For an ideal isotropic poroelastic material,

$$\alpha = 1 - \frac{K_{\mathrm{d}}}{K_{\mathrm{s}}} \tag{5}$$

with K_{d} being the drained bulk modulus of the material, and K_{s} that of the solid matrix (Detournay and Cheng, 1993). The constitutive relation between the variation of the fluid content ζ and stress is described by

$$2G_{\mathrm{d}}\zeta = \alpha\left(\frac{1 - 2v_{\mathrm{d}}}{1 + v_{\mathrm{d}}}\right)\left(\sigma_{kk} + \frac{3p}{B}\right), \tag{6}$$

where B is the compressibility or Skempton pore pressure coefficient (Cowin, 1999). B is defined by

(Detournay and Cheng, 1993)

$$B = \frac{\alpha K_{\mathrm{f}}}{[\alpha - \varphi(1 - \alpha)]K_{\mathrm{f}} + \varphi K_{\mathrm{d}}}, \tag{7}$$

where φ is the pore volume fraction and K_{f} the fluid bulk modulus.

The mechanical behaviour of a fluid-saturated medium is completely described by Eqs. (1)–(7). For their application to cortical bone, parameters must be quantified that describe the linear-elastic behaviour of bone (any two of E_{d}, v_{d}, G_{d}, and K_{d}), the porosity (φ), the compressibility of the fluid phase and the solid phase (K_{s} and K_{f}), and hydraulic permeability κ. Except for φ and K_{f} (taken from the literature), these parameters are derived below for both levels of porosity.

2. The isotropic elastic material parameters

Cortical bone has two levels of interconnected channels. First, the vascular level porosity (diameter $\sim 50\,\mu\mathrm{m}$; subscript v) consisting of the space occupied by the bone fluid in the Haversian and Volkmann canals. Second, the lacuno-canalicular level porosity (diameter $< 0.5\,\mu\mathrm{m}$; subscript lc) containing the osteocytes and extracellular bone fluid. As it is not possible to experimentally determine the elastic material constants of the solid matrix at these levels, a theoretical approach is presented, based on experimental data taken from literature. For reasons given earlier, the approach is limited to isotropic conditions.

Cowin and Sadegh (1991) constructed a set of effective isotropic elastic constants for human cortical bone, based on experimental orthotropic data from Ashman et al. (1984). It is assumed here that the vascular pores were no longer saturated, so the fluid pressure is zero. Consequently, the effective elastic

Table 1
Summary of the isotropic elastic constants for cortical bone on two levels of porosity[a]

Property (units, if any)	Vascular level	Lacuno-canalicular level
φ, porosity	*0.04*	*0.05*
K_f (GPa), bulk modulus of fluid	*2.3*	*2.3*
E_d (GPa), drained Young's modulus	*14.58*	15.75
v_d, drained Poisson's ratio	*0.325*	0.325
G_d (GPa), drained shear modulus	*5.50*	5.94
K_d (GPa), drained bulk modulus	*13.92*	14.99
E_s (GPa), solid Young's modulus	15.85	17.51
v_s, solid Poisson's ratio	0.333	0.335
G_s (GPa), solid shear modulus	5.94	6.56
K_s (Gpa), solid bulk modulus	15.82	17.66
E_u (GPa), undrained Young's modulus	14.65	15.85
v_u, undrained Poisson's ratio	0.332	0.333
G_u (GPa), undrained shear modulus	5.50	5.94
K_u (GPa), undrained bulk modulus	14.56	15.82
α, effective stress coefficient	0.120	0.151
B, Skempton pore pressure coefficient	0.367	0.344

[a] The values in italic were taken from Cowin (1999). The other elastic constants have been calculated from Eqs. (8)–(12). The expressions for α and B can be found in Detournay and Cheng (1993), p. 121 and 118, respectively.

constants are the drained elastic moduli at the vascular level: $K_{d,v} = 13.92$ GPa, $G_{d,v} = 5.50$ GPa, $E_{d,v} = 14.58$ GPa, and $v_{d,v} = 0.325$ (Table 1). The vascular porosity $\varphi_v = 0.04$ (Zhang et al., 1998).

The theory of composite materials (Christensen, 1979) provides equations relating effective elastic constants of porous materials to the size and distribution of the pores and the elastic properties of the matrix material. The following relationships between the drained moduli ($K_{d,v}$ and $G_{d,v}$) and the solid phase moduli ($K_{s,v}$, $G_{s,v}$) are applications of equations in Christensen (1979) for spherical voids:

$$K_{d,v} = K_{s,v} - \frac{K_{s,v}\varphi}{1 - K_{s,v}/(K_{s,v} + (4/3)G_{s,v})} \tag{8}$$

and

$$\frac{G_{d,v}}{G_{s,v}} = 1 - \frac{15(1 - v_{s,v})\varphi}{7 - 5v_{s,v}}. \tag{9}$$

Further, for all isotropic linear elastic materials,

$$\frac{K_{s,v}}{G_{s,v}} = \frac{2(1 + v_{s,v})}{3(1 - 2v_{s,v})}. \tag{10}$$

Using (8)–(10), the unknowns $K_{s,v}$, $G_{s,v}$ and $v_{s,v}$, as well as $E_{s,v}$ are determined: $K_{s,v} = 15.82$ GPa; $G_{s,v} = 5.94$ GPa; $v_{s,v} = 0.333$; and $E_{s,v} = 15.85$ GPa (Table 1).

The elastic constants of the porous bone material at the lacuno-canalicular level can be determined similarly. As the experiments by Ashman et al. (1984) were performed with ultrasound (2.25 MHz), and the relaxation time of the lacuno-canalicular fluid pressure is of the order of 0.1–3.0 s (Pienkowski and Pollack, 1983; Otter et al., 1992), the porous structure is now considered *undrained*. Consequently, the undrained elastic moduli for the porous medium at the lacuno-canalicular level equals the elastic moduli for the solid material at the vascular level ($K_{u,lc} = K_{s,v}$; $G_{u,lc} = G_{s,v}$; $v_{u,lc} = v_{s,v}$; $E_{u,lc} = E_{s,v}$). Detournay and Cheng (1993) give the following relationships between undrained, drained and solid elastic moduli:

$$K_u = K_d \left[1 + \frac{(1 - K_d/K_s)^2}{K_d/K_s(1 - K_d/K_s) + \varphi(K_d/K_f - K_d/K_s)} \right] \tag{11}$$

and

$$v_u = \frac{3K_u - 2G_d}{2(3K_u + G_d)}. \tag{12}$$

Combining (11) with (8), and (12) with (9) and (10), two expressions for K_u are obtained with two unknowns, K_s and v_s. With $\varphi_{lc} = 0.05$ (Zhang et al., 1998), the elastic moduli for the solid material at the lacuno-canalicular level are: $K_{s,lc} = 17.66$ GPa; $G_{s,lc} = 6.56$ GPa; $v_{s,lc} = 0.335$; and $E_{s,lc} = 17.51$ GPa. Using (8)–(10), the drained elastic moduli become: $K_{d,lc} = 14.99$ GPa; $G_{d,lc} = 5.94$ GPa; $v_{d,lc} = 0.325$; and $E_{d,lc} = 15.75$ GPa. Note that the solid moduli are higher at levels of lower porosity: $K_{s,bone} < K_{s,v} < K_{s,lc}$.

Many other parameters can be used to describe the poroelastic problem, such as the effective stress coefficient α (Nur and Byerlee, 1971). Also, the Skempton pore pressure coefficient B and the undrained elastic material properties can be calculated if a value for the bulk modulus of the contents of the porosities is assumed (Detournay and Cheng, 1993). Table 1 gives a summary of these.

3. The hydraulic permeability of the lacuno-canalicular network

In porous media, fluid flow depends on the pressure gradient, fluid viscosity μ, and the structure of the porosity, expressed as intrinsic permeability k. k depends on the number, orientation and size of the canaliculi, as well as on the amount of filling by osteocytes and their processes. These parameters are
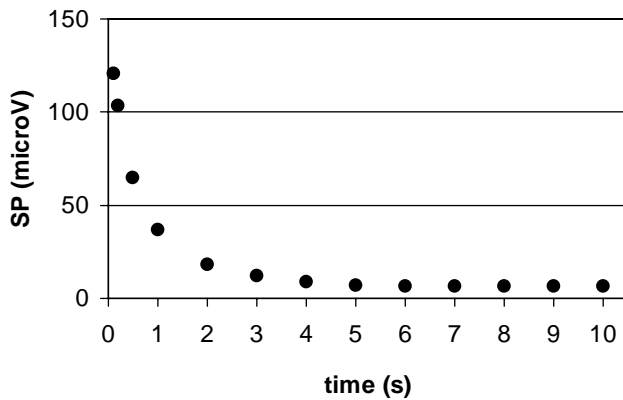
Fig. 1. Relaxation curve of the streaming potentials after step loading recorded in a dog's femur in vivo. Adapted from Otter et al. (1992).

very difficult to determine, leading to estimations of permeability k ranging over several orders of magnitude (Wang et al., 1999). Therefore, a more direct approach is chosen to estimate the hydraulic permeability κ, which includes both the intrinsic (geometrical) permeability k and the fluid viscosity μ ($\kappa = k/\mu$).

In a porous structure loaded by a step-function, fluid is pressurised at $t = 0$, and then relaxes due to drainage; in osteonic bone, extracellular fluid drains into the Haversian canals (Starckebaum et al., 1979; Iannacone et al., 1979). The relaxation curve is basically a function of the osteonic dimensions; the material properties of the solid bone matrix and the extracellular fluid; the porosity of the bone matrix; and the hydraulic permeability of the system. Except for the hydraulic permeability, all these parameters can be estimated using data from the literature or Section 2. Hydraulic permeability then can be estimated with the use of a finite element model of an osteon, by relating the calculated step response with an experimentally determined relaxation curve. For this study, we compare with the relaxation curve of streaming potentials recorded in vivo in a dog femur (Otter et al., 1992) (Fig. 1).

An axisymmetric finite element model of an osteon was built with an inner and outer radii of 12.5 and $80 \, \mu m$, respectively. These are characteristic dimensions of an osteon in a dog's femur (Jowsey, 1966). The finite element code DIANA (TNO, The Netherlands) requires the drained Young's modulus ($E_{d,lc} = 15.75 \, \text{GPa}$) and Poisson's ratio ($v_{d,lc} = 0.325$); the lacuno-canalicular bone porosity ($\varphi_{lc} = 0.05$; Zhang et al., 1998); the bulk moduli of the solid matrix ($K_{s,lc} = 17.66 \, \text{GPa}$) and the extracellular fluid ($K_f = 2.3 \, \text{GPa}$; Anderson, 1967); and the hydraulic permeability, the value of which is to be determined.

Based on experiments by Starckebaum et al. (1979), Iannacone et al. (1979) and Otter et al. (1994), it is assumed that every osteon is a draining system on its own. Consequently, the outer boundary is considered
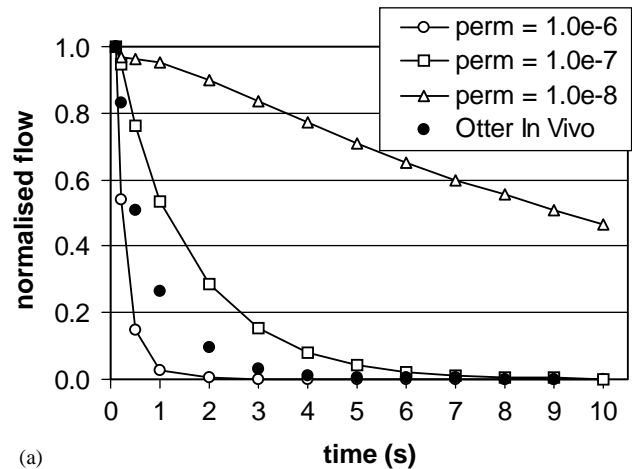
(a)
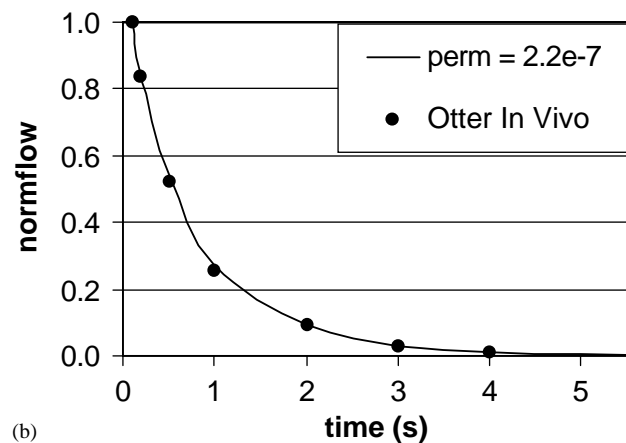
(b)

Fig. 2. (a) Relaxation of the normalised pressure difference between the inner and outer osteon border for different values of the hydraulic permeability κ. The experimental relaxation curve by Otter et al. runs between the curves for $\kappa = 10^{-6}$ and $10^{-7} \, \text{mm}^4/\text{N s}$. (b) Further refinement results in an estimation of the hydraulic permeability $\kappa = 2.2 \times 10^{-7} \, \text{mm}^4/\text{N s}$.

impermeable. The cylinder is further considered to be infinitely long, so only the surface of the Haversian canal is open for drainage. The reference pressure within the channel was set to zero (Cowin, 1999), and an axial compressive step load was applied resulting in a deformation of 1000 µstrain. The model was analysed with $\kappa = 10^{-6} \, \text{mm}^4/\text{N s}$, $\kappa = 10^{-7} \, \text{mm}^4/\text{N s}$, and $\kappa = 10^{-8} \, \text{mm}^4/\text{N s}$. The estimation was subsequently refined in analyses with intermediate values. As drainage of bone fluid is considered to occur exclusively through the lacuno-canalicular network into the Haversian canal, the relaxation of the streaming potential determined by Otter et al. is proportional to the relaxation of the pressure gradient over the osteonic wall.

Fig. 2 shows the normalised pressure drop, with unity at $t = 0.1 \, \text{s}$. Note that the experimentally determined relaxation curve by Otter et al. has an offset of $\sim 7 \, \mu V$
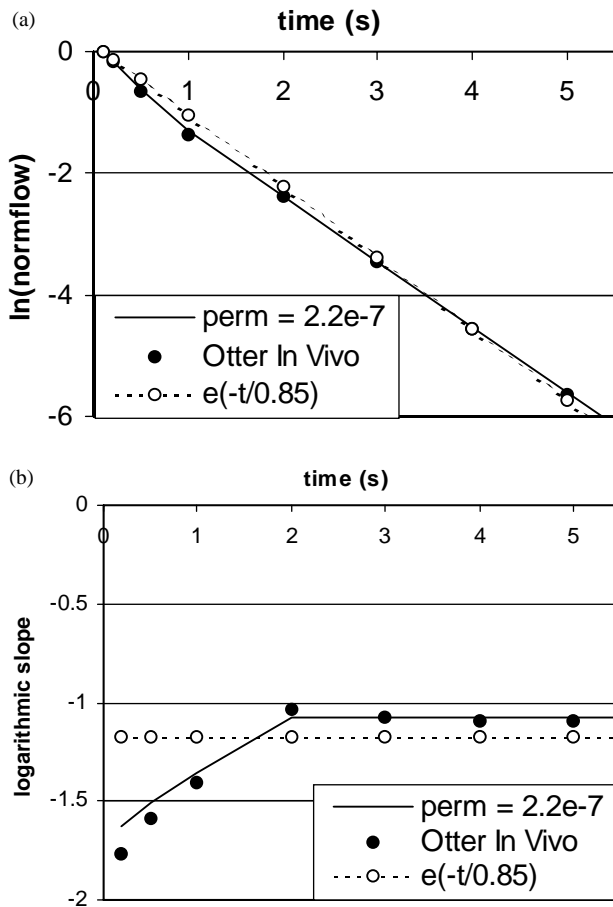
Fig. 3. (a) The experimental and numerical curves on a logarithmic scale are well approximated by a normalised negative e-power with a time constant $\tau_r = 0.85\,\text{s}$. (b) The slope of the logarithmic curves shows, however, that both the experimental and the numerical curve have time constants increasing from approximately $\tau_r = 0.60$ at $t = 0.1\,\text{s}$ to $\tau_r = 0.95\,\text{s}$ after $t = 2.0\,\text{s}$.
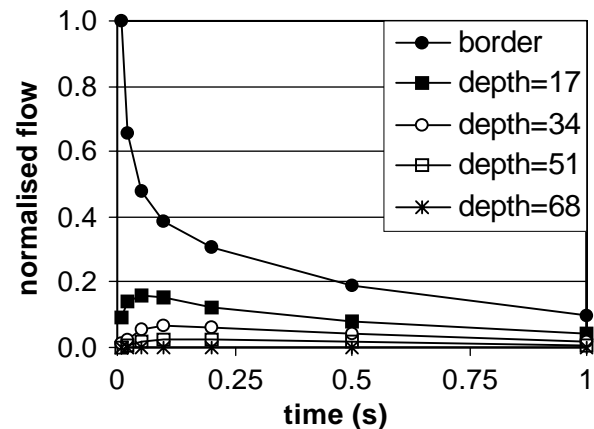

Fig. 4. Relaxation curves at different sites along the osteonic radial during the first second after loading. Note that the deeper sites start to relax later than the more superficial bone layers. Also note that most of the fluid flow occurs at the bone surface near the Haversian canal. Depths are in µm.

(Fig. 1); as no rheological reason exists for this threshold, this value is considered as a zeroing error, and subtracted from the normalised curve. Fig. 2a shows the experimental curve between the numerical curves for $\kappa = 10^{-6}$ and $10^{-7}\,\text{mm}^4/\text{N s}$. Further refinement results in an estimation of $\kappa = 2.2 \times 10^{-7}\,\text{mm}^4/\text{N s}$ (Fig. 2b). On a logarithmic (ln) scale, relaxation is described by an almost straight line, which is well approximated by a normalised negative e-power with time constant $\tau_r = 0.85\,\text{s}$ (Fig. 3a). However, the slope of the logarithmic relaxation function shows that there is not one single time constant, but—at least within the time frame up to 2 s—a shifting time constant (Fig. 3b). Kufahl and Saha (1990) explained this phenomenon by assuming that the deeper parts of the osteon relax more slowly than the superficial parts of the bone, which we found in our model as well (Fig. 4). The question of biphasic relaxation curve in pore fluid pressure is also measured and discussed in the work of Qin et al. (2001, 2002).

4. Discussion

The parameters for a double porosity isotropic Biot model of cortical bone were estimated using composite modelling and experimental data from literature. The theoretical part is based on the theory of poroelasticity (Biot, 1941; Detournay and Cheng, 1993), and contains two assumptions that have to be considered.

First, the two porosity levels in cortical bone are considered to act independently, because the pressure relaxation times differ by four orders of magnitude. This means that it is reasonable to assume that the bone matrix with the lacuno-canalicular network can be considered solid for the short time scale behaviour of the vascular porosity, and the pressure in the vascular porosity does not interfere with the fluid flow within the lacuno-canalicular network. The relaxation of the streaming potentials measured by Otter et al. (1992) is assumed to originate from the lacuno-canalicular network only, as the pressure within the vascular porosities must be completely relaxed after about 100 µs.

The second assumption is isotropy. For the elasticity parameters, this is justified even for lamellar bone (Cowin and Sadegh, 1991), but permeability must differ considerably between longitudinal and radial directions; transverse and longitudinal sections of lamellar cortical bone give the impression that canaliculi mainly run radially towards the Haversian canals (Gray's Anatomy, 1995). With the axisymmetric approach in the finite element analysis, the estimated permeability thus is in the transverse plane of the osteon.

The value for the hydraulic permeability estimated in this study ($\kappa = 2.2 \times 10^{-7}\,\text{mm}^4/\text{N s}$) is two orders of magnitude smaller than those used in studies by Zhang et al. (1998) and Wang et al. (1999). These authors based

their estimation on geometrical parameters of the porosity, the values of which are in fact highly uncertain. One physical explanation for this discrepancy could be that the degree of filling of the canaliculi by the osteocytic processes was underestimated, or in other words, the fluid layer between the cellular processes and the bone matrix is less than that assumed by these authors (some 50 nm). This would fit with the findings by Petrov (2000) that the effective porosity radius in bone is of the order of 10 nm. Other possible explanations are that the viscosity or the number of canaliculi is higher. On the other hand, the present study also has debatable input values. Lacuno-canalicular porosity, for example, was assumed to be 5%, but has also been reported to be as low as 0.023 (in man; Frost, 1960) and 0.042 (in dogs; Morris et al., 1982). The poroelastic bone parameters and the hydraulic permeability, however, are not very sensitive to changes in the lacuno-canalicular porosity, that is, their values remain of the same order of magnitude (own unreported data; Zhang et al., 1998). The same holds for osteonic dimensions and the elastic moduli of the bone tissue. It should be noted, however, that the porosity of 5% refers to the whole lacuno-canalicular space, and includes both the cells and the freely flowing fluid. Cells and fluid are combined here because of their comparable bulk modulus, as opposed to the bulk modulus of the mineralised matrix. The absolute fluid flow thus will be higher than calculated with the model presented, because a part of the porosity contents does not flow. The estimated hydraulic permeability, however, does not change because it has been derived directly from the relaxation times, not from the geometrical dimensions of the canaliculi and osteocytic protrusions.

It is interesting to note that the essentials of the relaxation curve recorded in vivo by Otter et al. can be approximated with a simple finite element model of fluid flow in an osteon under axial step compression. Especially, the observation that the relaxation curve is described by a shifting time constant due to the later response of the deeper osteon layers, strongly suggests that the streaming potentials measured by Otter et al. are due to canalicular fluid flow *only*, and do not require a pathway through or an exchange with the bone's microporosity, as suggested by others (Salzstein et al., 1987; Pollack and Petrov, 2000; Petrov and Pollack, 2000). This hypothesis is consistent with observations by Otter et al. (1994) that the bone fluid mainly drains into the Haversian canals.

Finally, it must be considered that cortical bone may show a wide variety of elastic moduli, permeabilities and osteonal dimensions for functional reasons. It is conceivable, for example, that the human skull has different values as compared to the rest of the skeleton. In this context, it is also interesting to consider that osteonic dimensions differ with species (Jowsey, 1966; Albu et al., 1990), but also differ within the same animal (Skedros et al., 1997). What this means for the mechanosensitivity of their bone tissue is an interesting area of research.

Acknowledgements

References

Albu, I., Georgia, R., Georoceanu, M., 1990. The canal system in the diaphysial compacta of the femur in some mammals. Anatomischer Anzeiger 170, 181–187.

Anderson, C.B., 1967. Mechanics of fluids. In: Baumeister, T. (Ed.), Marks' Saturated Handbook for Mechanical Engineers, pp. 3.24–3.76. McGraw-Hill, New York.

Ashman, R.B., Cowin, S.C., Van Buskirk, W.C., Rice, J.C., 1984. A continuous wave technique for the measurement of elastic properties of cortical bone. Journal of Biomechanics 17, 349–361.

Biot, M.A., 1941. General theory of three-dimensional consolidation. Journal of Applied Physics 12, 155–164.

Biot, M.A., 1955. Theory of elasticity and consolidation for a porous anisotropic solid. Journal of Applied Physics 26, 182–185.

Burger, E.H., Klein Nulend, J., Cowin, S.C., 1998. Mechanotransduction in bone. In: Zaidi, M. (Ed.), Advances in Organ Biology, Vol. 5a, pp. 107–118. JAI Press, London.

Christensen, R.M., 1979. Mechanics of Composite Materials. Wiley, New York, pp. 41–47.

Cowin, S.C., 1999. Bone poroelasticity. Journal of Biomechanics 32, 217–238.

Cowin, S.C., Sadegh, A.M., 1991. Non-interacting modes for stress, strain and energy in hard tissue. Journal of Biomechanics 24, 859–867.

Cowin, S.C., Weinbaum, S., Zeng Yu, 1995. A case for bone canaliculi as the anatomical site of strain-generated potentials. Journal of Biomechanics 28, 1281–1296.

Detournay, E., Cheng, A.H.D., 1993. Fundamentals of poroelasticity. In: Hudson, J.A. (Ed.), Comprehensive Rock Engineering: Principles, Practice and Projects. Pergamon, Oxford, pp. 113–171.

Frost, H.M., 1960. Measurement of osteocytes per unit volume and volume components of osteocytes and canaliculi in man. Henry Ford Hospital Medical Bulletin 8, 208–211.

Gray's Anatomy, 1995. 38th Edition. Churchill Livingstone, New York.

Iannacone, W., Korostoff, E., Pollack, S.R., 1979. Microelectrode studies of stress-generated potentials obtained from uniform and nonuniform compression of human bone. Journal of Biomedical Materials Research 13, 753–763.

Jowsey, J., 1966. Studies of Haversian systems in man and some animals. Journal of Anatomy 100, 857–864.

Kufahl, R.H., Saha, S., 1990. A theoretical model for stress-generated fluid flow in the canaliculi-lacunae network in bone tissue. Journal of Biomechanics 23, 171–180.

Morris, M.A., Lopez-Curato, J.A., Hughes, S.P.F., An, K.N., Bassingthwaigthe, J.B., Kelly, P.J., 1982. Fluid spaces in canine bone and marrow. Microvascular Research 23, 188–200.

Nur, A., Byerlee, J.D., 1971. An exact effective stress-strain law for elastic deformation of rock with fluids. Journal of Geophysical Research 76, 6414–6419.

Otter, W.M., Palmieri, V.R., Wu, D.D., Seiz, K.G., MacGinitie, L.A., Cochran, G.V.B., 1992. A comparative analysis of streaming potentials in vivo and in vitro. Journal of Orthopaedic Research 10, 710–719.

Otter, M.W., MacGinitie, L.A., Seiz, K.G., Johnson, M.W., Dell, R.B., Cochran, G.V.B., 1994. Dependence of streaming potential frequency response on sample thickness: implication for fluid flow through bone microstructure. Biomemetics 2, 57–75.

Petrov, N., 2000. Estimation of the hydraulic canalicular radius in cortical bone. Journal of Theoretical Applied Mechanics 30, 84–92.

Petrov, N., Pollack, S.R., 2000. An anatomical model of stress induced fluid flow in osteons. Proceedings of the International Conference on Biorheology, Sofia 2000.

Piekarski, K., Munro, M., 1977. Transport mechanism operating between blood supply and osteocytes in long bones. Nature 269, 80–82.

Pienkowski, D., Pollack, S.R., 1983. The origin of stress generated potentials in fluid saturated bone. Journal of Orthopaedic Research 1, 30–41.

Pollack, S.R., Petrov, N., 2000. A triple porosity model of stress induced fluid flow in cortical bone. Proceedings of the International Conference on Biorheology, Sofia 2000.

Qin, Y.-X., Lin, W., Rubin, C.T., 2001. Load-induced intracortical flow pathway and its potential role in bone adaptation. Proceedings of the Bioengineering Conference, American Society of Mechanical Engineers, Bioengineering Division 50, 337.

Qin, Y.-X., Lin, W., Rubin, C.T., 2002. The pathway of load-induced bone fluid flow as defined by in vivo intramedullary pressure and streaming potentials. Measurements, Annals of Biomedical Engineering, in revision.

Salzstein, R.A., Pollack, S.R., Mak, A.F.T., Petrov, N., 1987. Electromechanical potentials in cortical bone—I. A continuum approach. Journal of Biomechanics 20, 261–270.

Skedros, J.G., Su, S.C., Bloebaum, R.D., 1997. Biomechanical implications of mineral content and microstructural variations in cortical bone of horse, elk, and sheep calcanei. Anatomical Record 249, 287–316.

Starckebaum, W., Pollack, S.R., Korostoff, E., 1979. Microelectrode studies of stress-generated potentials in four-point bending of bone. Journal of Biomedical Materials Research 13, 729–751.

Wang, L., Fritton, S.P., Cowin, S.C., Weinbaum, S., 1999. Fluid pressure relaxation depends on osteonal microstructure: modeling an oscillatory bending experiment. Journal of Biomechanics 32, 663–672.

Wang, L., Cowin, S.C., Weinbaum, S., Fritton, S.P., 2000. Modeling tracer transport in an osteon under cyclic loading ann. Biomedical Engineering. 28, 1200–1209.

Weinbaum, S., Cowin, S.C., Zeng, Y., 1991. A model for the fluid shear stress excitation of membrane ion channels in osteocytic processes due to bone strain. In: Vanderby, R. (Ed.), Advances in Bioengineering. American Society of Mechanical Engineers, New York, pp. 317–320.

Zhang, D., Weinbaum, S., Cowin, .S.C., 1998. Estimates of the peak pressures in bone pore water. Journal of Biomechanical Engineering 120, 697–703.